ChemComm

COMMUNICATION

View Article Online
View Journal | View Issue

Cite this: *Chem. Commun.*, 2018, **54**, 12770

Received 10th October 2018,
Accepted 22nd October 2018

DOI: 10.1039/c8cc08099b

rsc.li/chemcomm

Light-induced desorption of trivalent chromium from adsorbents: one step closer to sustainability†

Xiaoyu Guan,[a] Sunxian Yan,[a] Jinming Chang,[a] Gaofu Yang[a] and Haojun Fan*[ab]

The environmental sustainability of existing adsorbents in remediating chromium-contaminated water has long been plagued by the necessity of using chemical desorbents in regenerating the adsorbents. Here, we demonstrate that trivalent chromium can be repelled from surface-bound merocyanine upon visible-light irradiation, avoiding any chemical desorbent, and thus secondary contamination, to restore the adsorption capacity of the exhausted adsorbents.

Since the last decade, concerns over contamination of aquatic ecosystems from the worldwide use of chromium in anthropogenic activities have been escalating.[1,2] This stimulates interest in developing 'end-of-pipe' techniques that enable efficient removal of chromium contaminants from water before it was disposed of or delivered. One of the most promising alternatives is adsorption,[3] the majority of which employs solid surfaces with immobilized organic ligands to capture soluble chromium species.[4,5] In recent years, there has been a surge of publications on new adsorbents suitable for remediating chromium-contaminated water.[6–8] These adsorbents are highly efficient, readily separable, and sometimes chromium selective. In addition, virtually all previous studies highlight regenerability of the designed adsorbents, by which the adsorption capacity of the exhausted adsorbents can be restored and any valuable chromium retained can be recovered. To date, regenerability has been an essential criterion to evaluate the performance and, in particular, cost effectiveness of a chromium-targeting adsorbent for up-scaling its application. However, to the best of our knowledge, the adsorbents reported previously unexceptionally require strong acids, alkalis, or chelating agents to sequester the chromium ions.[4,6,8] Indeed, discharging effluents containing chemical desorbents themselves contribute to secondary contamination, a long-ignored problem that compromises sustainability of adsorption techniques in remediating chromium-containing water.

Ideally, an environmentally sound adsorbent should exhibit high efficiency to capture chromium species in aqueous solution, while being capable of desorbing the retained chromium on demand without mechanical or chemical disruption. Recent advances in stimuli-responsive materials provide a unique opportunity to address this challenge. By virtue of high spatiotemporal resolution of light, photoswitchable compounds able to reversibly undergo light-induced transitions between two or more metastable states with different physicochemical properties have been the current focus of attention for a wide spectrum of emerging applications.[9,10] Among others, spiropyrans are an important class of photoswitchable compounds. Spiropyran features an indole and a benzopyran moiety, jointed together at the spiro sp^3-hybridized carbon atom leading to a perpendicular orientation of both the planar heterocyclic rings. Upon exposure to visible light, the spiropyran exists in a charge-neutral, colorless, and closed form (SP), which isomerizes to the corresponding zwitterionic, colored merocyanine (MC) form *via* heterolytic cleavage of the spiro carbon–oxygen bond upon UV irradiation, by metal ions or by polar solvent stimulus.[11] Here, it is noted that a phenolate group is generated once the SP photoisomerizes to the MC species. As long as the phenolate in MC remains deprotonated, the negatively charged phenoxy oxygen can operate as a ligand to interact with electronically poor species such as chromium cations. More importantly, since the MC → SP ring-closing reaction is reversible under visible light, we envision that irradiation with visible light may liberate the chromium cations back into the aqueous media, leading to regeneration of the adsorbents in a photo-controllable manner. The feasibility of this strategy has been demonstrated preliminarily in the present study by using a spiropyran derivative covalently immobilized onto two representative solid surfaces, *i.e.*, silicon wafer (SW) and magnetite particles (Fe_3O_4). Since light is a noninvasive and environmentally benign stimulus with high spatiotemporal solution, the rationale underlying the present effort may provide guidance for designing new adsorbents that

[a] *Key Laboratory of Leather Chemistry and Engineering of Ministry of Education, Sichuan University, Chengdu 610065, P. R. China*
[b] *State Key Laboratory of Polymer Materials Engineering, Sichuan University, Chengdu, 610065, P. R. China. E-mail: fanhaojun@scu.edu.cn*

† Electronic supplementary information (ESI) available. See DOI: 10.1039/c8cc08099b

address the aforementioned contamination associated with the use of chemical desorbents, a universal problem that has not been solved yet in remediating chromium-containing water by adsorption.

To covalently immobilize spiropyran onto SW and Fe_3O_4, a spiropyran with a propionic acid side chain appended to the indolic nitrogen was synthesized (ESI,† Scheme S1) according to a previously disclosed procedure.[12] The chemical structure of the product was verified by Fourier transform infrared (FTIR) spectroscopy, ^{1}H nuclear magnetic resonance (NMR) spectroscopy, and electrospray ionization mass spectrometry (ESI-MS) (ESI,† Fig. S1–S6). The appended propionic acid acted as a reactive point for covalent immobilization of the spiropyran derivative onto solid surfaces. In addition to the phenolate produced by the heterolytic cleavage of the spiro carbon–oxygen bond, there were no other ligands (*e.g.*, the hydroxyl group in the vicinity of the phenolate group) in the spiropyran derivative; otherwise extra ligands bond irreversibly with trivalent chromium that could not be photochemically repelled from the adsorbents. Then, a DMF (dimethylformamide)/H_2O solution (50 : 50 v/v) of the spiropyran derivative at a concentration of 2.5×10^{-4} M was prepared. After stored in the dark for 240 min, 38% of the spiropyran derivative isomerized into the ring-opened MC form (ESI,† Fig. S7). Accordingly, the colorless solution turned red, accompanied by the appearance of an intense absorption band in the visible region with the peak maximum at 530 nm (Fig. 1(a)). Upon the addition of Cr(III) (2.5×10^{-4} M) into the MC solution, a new absorption peak at 420 nm appeared while the absorption at 530 nm experienced a red shift as a function of time (Fig. 1(b)), indicating the formation of an MC–Cr(III) complex.[13–15] Furthermore, based on Job's method of continuous variation (Fig. 1(c)) and Benesi–Hildebrand equation (Fig. 1(d)), the complex-ratio and the binding constant k of the MC–Cr(III) complex were calculated to be 0.45 and 5.3×10^3 M^{-1}, respectively, indicating that MC coordinates mildly with Cr(III) in a 1 : 1 stoichiometry (see the ESI†). Such an SP → MC transition was reversible, with *ca.* 88% (ESI,† Fig. S7) of the spiropyran molecules existing in the closed SP form after irradiation with visible light ($\lambda > 400$ nm) for 20 min (ESI,† Fig. S8). Accordingly, the UV-Vis absorption spectra of the mixture shifted back to the original state, with only one absorption detected in the visible region (ESI,† Fig. S8). This result indicated that the Cr(III) species were repelled from the spiropyran derivative as the MC photoisomerized to SP.

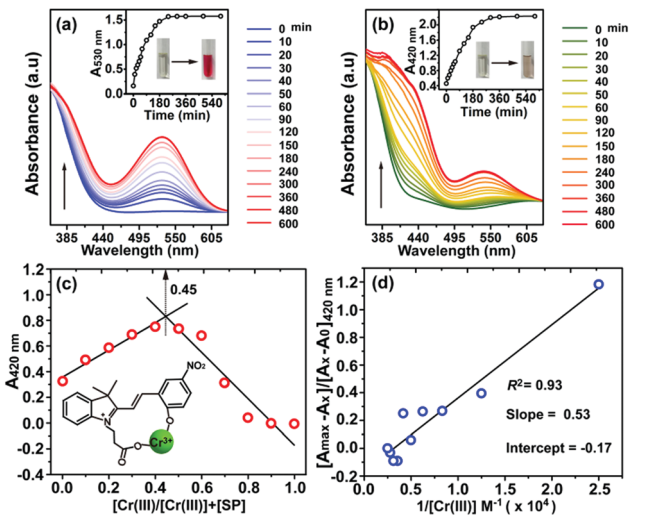

Fig. 1 UV-Vis absorbance spectra of (a) a spiropyran derivative (2.5×10^{-4} M) in DMF/H_2O solution (50 : 50 v/v, 293 K) and (b) after the addition of 1 equivalent of trivalent chromium under dark conditions; the inset shows their absorbance and solution color change over time. (c) Job's plot (total concentration of MC (SP) and trivalent chromium: 4×10^{-4} M) and (d) Benesi–Hildebrand plot of MC with trivalent chromium.

Then, the spiropyran derivate was covalently immobilized onto two representative solid surfaces, *i.e.*, amine-functionalized planar silicon wafer (SW) and spherical magnetite particles (Fe_3O_4) by EDC/NHS-mediated coupling, yielding two solid adsorbents SP@SW and SP@Fe_3O_4, respectively (Scheme 1). The successful immobilization of SP onto SW and the Fe_3O_4 surface was confirmed using various technologies. As for the synthesized SP@SW, compared with freshly cleaned SW (ESI,† Fig. S9), it was found that many small mountain-like protuberances were present on the SW surface, displaying a mean surface coating of 100 nm (Fig. 2(a)). Especially, the successful introduction of SP moieties on the SW outmost layer was systematically corroborated by (1) the ATR-FTIR spectrum (Fig. 2(b)) that amplified the 1450–1668 cm^{-1} region and made deconvolution of the interest displaying amide I (peak at 1654 cm^{-1}), amide II (peaks at 1554 and 1510 cm^{-1}, respectively) and Ar–NO_2 (peak at 1330 cm^{-1}) absorption bands, corresponding to the coupling amide bonds and 4-nitrophenyl from the chromene moiety, respectively; (2) the high-resolution XPS spectral envelopes (Fig. 2(d)) of (d_1) C 1s, (d_2) N 1s and (d_3) O 1s, simultaneously detecting the SP-derived C═O, C–O, N–O, and C═C signals; and (3) fluorescence microscopy imaging (Fig. 2(c)) demonstrating a red glow on the SW surface, attributing to the SP moieties that translate to a red color MC form under UV irradiation (ESI,† Fig. S10). In addition, UV-Vis absorbance analysis of the supernatant obtained from a residuary reaction mixture of the amide couplings showed that ~58.5 wt% of the added SP were attached onto the SW surface. The quantity of SP moieties immobilized onto the surface of SW was therefore calculated to be 72 mmol m^{-2}. Also, the successful synthesis of SP@Fe_3O_4 was characterized using SEM, TEM, XPS, and UV-Vis absorbance technologies (ESI,† Fig. S11 and S12), and the quantity of SP moieties immobilized onto the engineered Fe_3O_4 surface was 0.21 mg mg^{-1}.

Light-induced translocation of trivalent chromium (Cr(III)) around SP@SW and SP@Fe_3O_4 was then examined by exposing one piece ($10 \times 10 \times 0.6$ mm^3) of SP@SW or 150 mg of SP@Fe_3O_4 to 20 mL of Cr(III) solution with an initial concentration of 20 mg L^{-1} (see the ESI,† Fig. S13) in a thermostatic shaker. The mixture was agitated at 20 °C in the dark with a flow of ultrapure N_2 for 4 h. After that, the exhausted adsorbents were withdrawn, washed repeatedly with water, and then exposed to 10 mL of deoxygenized water under visible light (>400 nm) with vigorous stirring for 30 min (see the ESI,† Fig. S14) for desorbing Cr(III). Evidence supporting that Cr(III)

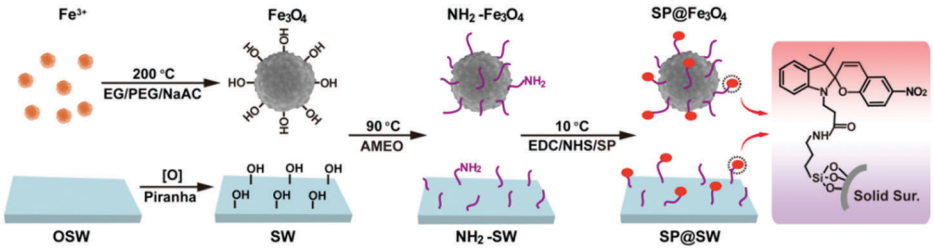

Scheme 1 Synthesis and structure of the representative solid adsorbents, SP@Fe_3O_4 and SP@SW.

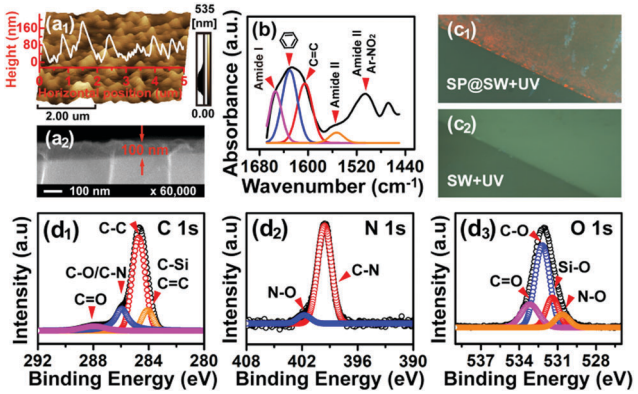

Fig. 2 (a_1) AFM height image (cross-sections were taken at the place indicated by the straight line), (a_2) SEM cross-section image, (b) ATR-FTIR spectrum, (c) fluorescence microscopy image, and (d_1) C 1s, (d_2) N 1s and (d_3) O 1s high-resolution XPS spectral envelopes of SP@SW. The deconvolved ATR-FTIR spectra were fitted with Gaussian band shapes *via* an iterative curve fitting procedure. To separate different species of the same element, a CasaXPS processing software was employed to deconvolve the XPS signals with a Gaussian–Lorentzian function (Gaussian = 80%, Lorentzian = 20%) after subtraction of a Shirley background.

was successfully adsorbed under dark conditions was provided by studies of SEM-EDS Cr-mapping and XPS of the exhausted SP@SW and SP@Fe_3O_4. As illustrated in Fig. 3 (b_1 and b_2, after treatment under dark conditions), the Cr element distributed evenly on the surface of the exhausted adsorbents. Accordingly, the high-resolution Cr 2p XPS spectrum (Fig. 3; c_1 and c_2, after treatment under dark conditions) revealed two signals, with BE peaks at 576.5/587 eV for SP@SW and 577.2/586.9 eV for SP@Fe_3O_4, corresponding to the Cr(III) element.[16,17] In comparison with the control (Fig. 2(d_2) and ESI,† Fig. S12(d_2)), the deconvolution of the N 1s spectral envelop (Fig. 3; c_1 and c_2, after treatment under dark conditions) revealed an extra component with BE peaks at 400.9 eV for SP@SW and 400.2 eV for SP@Fe_3O_4, ascribed to N^+ from the indoline moiety.[16] In the case of the regenerated adsorbents, the N^+ component disappeared in the corresponding N 1s spectral envelop (Fig. 3; c_1 and c_2, after Vis treatment), indicating that the MC moieties were transformed into the SP form. However, the Cr signal still appeared in the SEM-EDS Cr-mapping (Fig. 3; b_1 and b_2, after Vis treatment) and Cr 2p XPS spectra (Fig. 3; c_1 and c_2, after Vis treatment). Furthermore, to quantify the photo-mediated Cr(III) translocation around the adsorbents, the Cr(III) concentration in the residual solution was determined *via* ICP-OES, and the results are presented in Fig. 3(a). The adsorption capacity of the two adsorbents for Cr(III) was measured to be 0.88 g m^{-2} of SP@SW and 1.54 mg g^{-1} of SP@Fe_3O_4, respectively. After irradiation of the exhausted SP@SW and SP@Fe_3O_4 with visible light, there were still adsorbed-Cr(III) remaining on their surface (Fig. 3(a)), coinciding well with the SEM-EDS Cr-mapping and Cr 2p XPS results. The residual Cr(III) on the solid adsorbent surface (0.49 mg g^{-1} for SP@Fe_3O_4, while 0.61 g m^{-2} for SP@SW; Fig. 3(a)) may be ascribed to the physical interaction, which cannot be desorbed by visible light irradiation or chemical desorbents. Furthermore, in order to evaluate the binding capacity of the present designed adsorbents to other metal ions (M^{n+}), five M^{n+} with different valences, *i.e.*, K^+, Na^+, Pb^{2+}, Ca^{2+}, and Fe^{3+}, were also employed (ESI,† Fig. S15 and S16). Taking SP@Fe_3O_4 for the target adsorbent, the results showed that the relative amount of M^{3+} released from SP@Fe_3O_4 composites by visible light irradiation was the largest compared with those of M^+ and M^{2+} (ESI,† Fig. S16), indicating that efficient light-driven composite-regeneration was achieved with moderately stable complexes (M^{3+}[MC-moiety]), rather than with unstable (M^+[MC-moiety]) or very stable complexes (M^{2+}[MC-moiety]). Such results further confirmed that present adsorbents with a surface-bond spiropyran moiety were suitable to treat M^{3+}-contaminated water, exemplified by Cr^{3+}, realizing the regeneration of the adsorbents in a photo-controllable manner.

Subsequently, repeated regeneration of the exhausted adsorbents was carried out. The gradual decay of the adsorption capability for both adsorbents could be ascribed to photodegradation of those immobilized SP. In particular, ~27% (SP@SW) and ~14% (SP@Fe_3O_4) of immobilized SP photo-degraded after three switching cycles (ESI,† Fig. S17), calculated from the change in adsorption capability of chromium. However, it seemed like photodegradation did not occur for those free SP counterparts in DMF/H_2O solution under the same conditions (ESI,† Fig. S18). As documented previously,[11,18,19] immobilized SP has numerous advantages over the free counterpart including reduced photodegradation. The present results are inconsistent with the prediction, and a precise reason for this observation is still open to debate.

In conclusion, we demonstrate that light-induced, reversible isomerization of surface-bound spiropyran can be harnessed to desorb trivalent chromium. Since visible light is a noninvasive and environmentally benign stimulus with high spatiotemporal solution, the rationale underlying the present effort may provide guidance for designing new adsorbents that address secondary contamination derived from chemical desorbents,

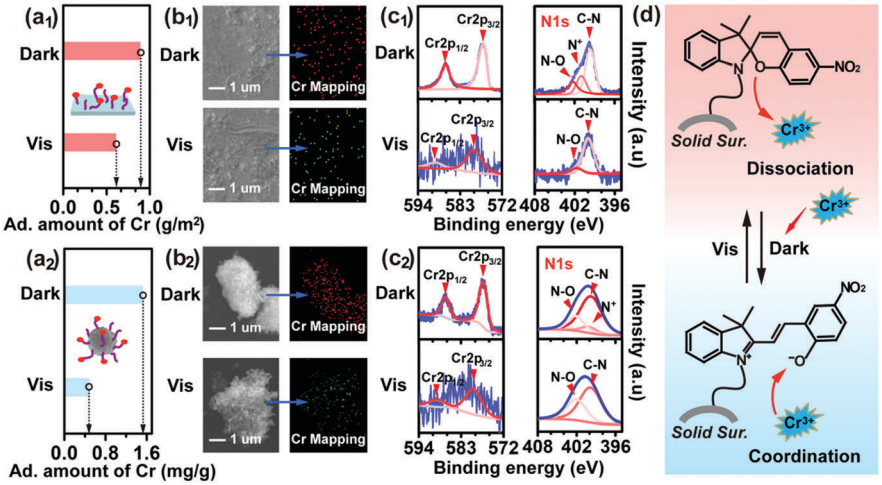

Fig. 3 (a) Adsorption (Ad.) amount of Cr, (b) zero-loss SEM image and the corresponding EDS Cr-mapping, and (c) Cr 2p and N 1s high-resolution XPS spectra of SP@SW (a_1, b_1 and c_1) and SP@Fe_3O_4 (a_2, b_2 and c_2) during the first recycling under the dark and irradiation by visible light (Vis), respectively. (d) Mechanism proposed for Cr(III) reversible photocontrollable coordination–dissociation by the solid adsorbents. A CasaXPS processing software was employed to deconvolve the XPS signals with a Gaussian–Lorentzian function (Gaussian = 80%, Lorentzian = 20%) after subtraction of a Shirley background.

bringing adsorption techniques one step closer to sustainability in treating chromium-contaminated water.

The authors gratefully acknowledge financial support of this work from the National Key Research and Development Program of China (2017YFB0308600), the National Natural Science Foundation of China (21576172), and the Fundamental Research Funds for the Central Universities (2012017yjsy177). We also thank Zhonghui Wang (College of Light Industry, Textile and Food Engineering, Sichuan University) for her help in conducting ICP-OES experiments, and Hui Wang (Analytical & Testing Center, Sichuan University) for help in SEM-EDS analysis.

Conflicts of interest

The authors declare no competing financial interests.

Notes and references

1 S. A. Cavaco, S. Fernandes, M. M. Quina and L. M. Ferreira, *J. Hazard. Mater.*, 2007, **144**, 634–638.
2 V. Sarin and K. K. Pant, *Bioresour. Technol.*, 2006, **97**, 15–20.
3 J. H. Jung, J. H. Lee and S. Shinkai, *Chem. Soc. Rev.*, 2011, **40**, 4464–4474.
4 X. Guan, J. Chang, Y. Chen and H. Fan, *RSC Adv.*, 2015, **5**, 50126–50136.
5 X. Guan, Y. Chen and H. Fan, *ACS Appl. Mater. Interfaces*, 2017, **9**, 15525–15532.
6 S. Huang, C. Ma, Y. Liao, C. Min, P. Du, Y. Zhu and Y. Jiang, *React. Funct. Polym.*, 2016, **106**, 76–85.
7 Y. Ko, K. Choi, S. Lee, K. Jung, S. Hong, H. Mizuseki, J. Choi and W. Lee, *Water Res.*, 2018, **145**, 287–296.
8 A. S. K. Kumar, S. Jiang and W. Tseng, *J. Mater. Chem. A*, 2015, **3**, 7044–7057.
9 M. Natali and S. Giordani, *Chem. Soc. Rev.*, 2012, **41**, 4010–4029.
10 X. Lu, S. Guo, X. Tong, H. Xia and Y. Zhao, *Adv. Mater.*, 2017, **29**, 1606467.
11 R. Klajn, *Chem. Soc. Rev.*, 2014, **43**, 148–184.
12 D. Liu, W. Chen, K. Sun, K. Deng, W. Zhang, Z. Wang and X. Jiang, *Angew. Chem., Int. Ed.*, 2011, **50**, 4103–4107.
13 T. Suzuki, Y. Kawata, S. Kahata and T. Kato, *Chem. Commun.*, 2003, 2004–2005.
14 K. H. Fries, J. D. Driskell, S. Samanta and J. Locklin, *Anal. Chem.*, 2010, **82**, 3306–3314.
15 M. Natali, C. Aakeröy, J. Desper and S. Giordani, *Dalton Trans.*, 2010, **39**, 8269–8277.
16 H. Gu, S. B. Rapole, J. Sharma, Y. Huang, D. Cao, H. A. Colorado, Z. Luo, N. Haldolaarachchige, P. David, B. Walters, S. Wei and Z. Guo, *RSC Adv.*, 2012, **2**, 11007–11018.
17 Y. Li, S. Zhu, Q. Liu, Z. Chen, J. Gu, C. Zhu, T. Lu, D. Zhang and J. Ma, *Water Res.*, 2013, **47**, 4188–4197.
18 A. Radu, R. Byrne, N. Alhashimy, M. Fusaro, S. Scarmagnani and D. Diamond, *J. Photochem. Photobiol., A*, 2009, **206**, 109–115.
19 S. Scarmagnani, Z. Walsh, C. Slater, N. Alhashimy, B. Paull, M. Macka and D. Diamond, *J. Mater. Chem.*, 2008, **18**, 5063–5071.